

Test and Study on the Mechanical Properties of Rock under Dynamic Loading

Bin Dong

School of Civil Engineering, Henan Polytechnic University, Jiaozuo, 454000, P.R. China

*E-mail: bdong2125@163.com

Abstract

A 100 mm diameter split Hopkinson pressure bar apparatus is applied to research the mechanical properties of the rock under different impact pressures. The results show that under different impact pressures, the dynamic stress-strain curves of rocks are similar to each other and can be divided into four stages. The dynamic peak stress and maximum strain of rock are more sensitive to the change of impact pressures. With the increase of impact pressures, the dynamic peak strength and maximum strain of the sample have a corresponding increase.

Keywords

Rock; Dynamic Mechanical Properties; Split Hopkinson Pressure Bar.

1. Introduction

Rock is an aggregate composed of minerals or cuttings according to certain laws under geological action. Different rocks have different mechanical properties due to their different compositions and structures. At present, in some engineering practices, rock masses are disturbed by multiple impact loads. For example, the drilling and blasting excavation of the underground chamber, the blasting construction of the tunnel face and the disturbance of the mechanical excavation will impose a certain dynamic load on the rock mass. Under the dynamic load, the micro-cracks inside the rock will continue to increase and expand, and then penetrate each other to form macro-cracks [1-4]. Therefore, it is of great significance to study the mechanical properties of rocks under dynamic loads for engineering practices [5].

In recent decades, the research on the mechanical properties of rock-like materials under dynamic loads has received extensive attention from academia and engineering [6, 7]. In recent years, a series of research results in this field have been achieved [8-12]. In this paper, based on the above research results, based on the SHPB test system, dynamic shock compression tests are carried out on rocks to analyze the dynamic characteristics of rocks under dynamic loads, in order to provide theoretical guidance for relevant practical engineering problems.

2. Test System

Uniaxial Shock Compression Test on Rock Specimens Using Improved SHPB Test Device. The adopted 100 mm-diameter SHPB system is presented schematically in Fig. 1. The experimental system is composed of a dynamic system, an incident rod, a transmission rod, an absorption rod and a data acquisition system. The bullet, incident rod, transmission rod and absorption rod used in the test system are all 100mm in diameter, and are made of 40Cr alloy steel.

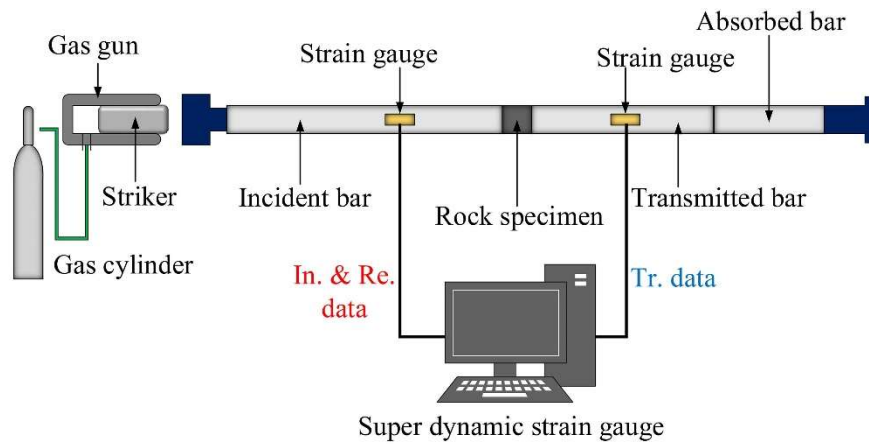


Fig. 1. Schsematic diagram of the SHPB system.

3. Specimen Preparation and Test Method

3.1 Specimen Preparation

The rock samples were collected from a sandstone mine, and sandstone samples with complete texture and good uniformity were selected as the research object. According to the rock mechanics test performance test regulations, the rock sample is processed and ground into a cylindrical sample of $\Phi 100\text{mm} \times 100\text{mm}$, and the non-parallelism and non-perpendicularity of the end face of the sample are both less than 0.02mm.

3.2 Test Principle

The SHPB test device is based on the assumption of one-dimensional stress wave and stress-strain uniformity, combined with the signals collected by the strain gauge during the test, and can calculate the dynamic stress, strain and strain rate according to the "three-wave method". The calculation formula is as follows [13, 14].

$$\sigma(t) = \frac{A_0}{2A_s} E_0 [\varepsilon_1(t) + \varepsilon_R(t) + \varepsilon_T(t)] \quad (1)$$

$$\varepsilon(t) = \frac{C_0}{L_S} \int_0^t [\varepsilon_1(t) - \varepsilon_R(t) - \varepsilon_T(t)] dt \quad (2)$$

$$\dot{\varepsilon}(t) = \frac{C_0}{L_S} [\varepsilon_1(t) - \varepsilon_R(t) - \varepsilon_T(t)] \quad (3)$$

In the formula, A_0 is the cross-sectional area of the compression bar, E_0 is the elastic modulus of the compression bar, C_0 is the 1D elastic bar wave speed, L_S is the length of the sample, A_S is the cross-sectional area of the sample.

If the stress in the sample changes uniformly and has no attenuation, it can be obtained from the one-dimensional stress wave theory that $\varepsilon_I(t) + \varepsilon_R(t) = \varepsilon_T(t)$, then the above formula can be simplified as follows:

$$\sigma(t) = \frac{A_0 E_0}{A_s} \varepsilon_T(t) \quad (4)$$

$$\varepsilon(t) = \frac{2C_0}{L_s} \int_0^t [\varepsilon_1(t) - \varepsilon_T(t)] dt \quad (5)$$

$$\dot{\varepsilon}(t) = \frac{2C_0}{L_s} [\varepsilon_1(t) - \varepsilon_T(t)] \quad (6)$$

3.3 Test Method

During the test, first move the incident rod and the transmission rod to the relative position, and then place the sample between the pressure bars. In order to reduce the end-face friction effect between the pressure rod and the contact surface of the sample, apply an appropriate amount of butter on the contact surface of the two ends of the sample and the pressure rod. Rock is a brittle material. In the SHPB test, the specimen often fails before reaching the stress balance. In order to prolong the rise time of the incident wave and effectively reduce the dispersion effect of the stress wave propagation, brass is used here.

During the test, align the pressure rod first and perform an empty flush, through multiple debugging, the shock air pressure reaches a stable state. During the test, the dynamic uniaxial compression test was carried out on the rock sample with four shock pressures of 0.20 MPa, 0.25 MPa, 0.30 MPa and 0.35 MPa, in order to explore the dynamic characteristics of the rock under dynamic load.

4. Analysis of Test Results

4.1 Stress-strain Curves and Dynamic Compressive Strength

The stress-strain curve of rock in dynamic test can comprehensively reflect the mechanical properties of the sample [15]. The dynamic stress-strain curve of rock under uniaxial shock compression state is shown in Fig. 2. As shown in Fig. 2, The dynamic stress-strain curves of rocks under different shock gas pressures have certain similarities. With the application of the impact load, the stress-strain curve of the specimen can be roughly divided into four stages, (1) At the initial stage of loading, the sample did not show an obvious compaction stage, but showed good elastic characteristics, and the stress increased uniformly with the increase of strain.. (2) With the propagation of the stress wave, the stress is in a flat stage and grows slowly with the increase of the strain. (3) At a certain time, the stress of the sample increases significantly with the increase of strain, and the growth rate remains basically unchanged. At this stage, the dynamic stress of the sample reaches the peak value. (4) At this stage, the dynamic stress of the specimen begins to decrease with the increase of strain, indicating that the rock has been damaged and the mechanical properties have deteriorated. In addition, with the increase of impact gas pressure, the opening amplitude of the stress-strain curve of the sample gradually increases, and the curve height also increases gradually.

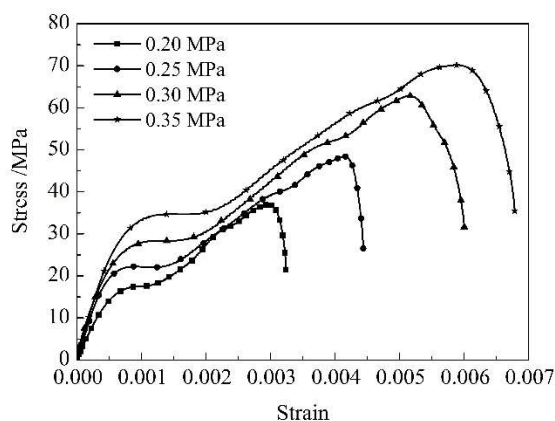


Fig. 2. Stress-strain curves of rock specimens.

4.2 Peak Stress

The dynamic peak stress variation law of rock under different shock pressure is shown in Fig. 3. It can be seen from the figure that with the increase of the shock gas pressure, the dynamic peak stress of the rock shows a gradually increasing trend, and the sample shows a strong correlation with the impact pressure. The reason for this phenomenon is mainly because the greater the impact pressure, the greater the energy provided, and the essence of rock damage is the transformation of energy. The larger impact gas pressure means that the sample can absorb more energy for the damage and failure of the rock itself, and the dynamic peak strength of the sample also increases accordingly.

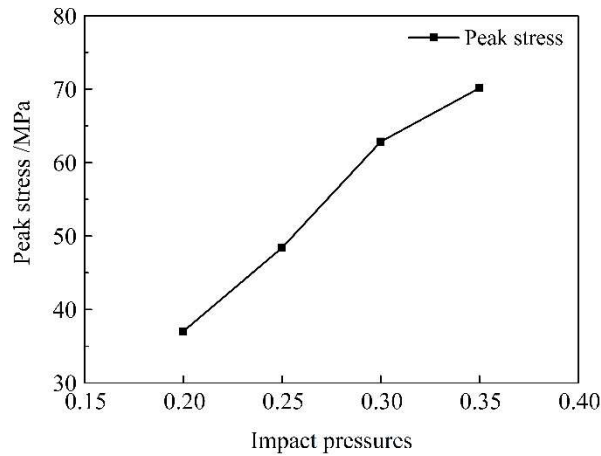


Fig. 3. Relationship between peak stress and impact pressures.

4.3 Maximum Strain

The strain of rock reflects the degree of internal deformation, and is one of the important research indicators for exploring rock dynamics. The rock was subjected to shock compression tests with different shock gas pressures, and the variation law of the maximum strain of the sample with the shock gas pressure during the dynamic loading process was obtained, as shown in Fig. 4. With the increase of shock impact pressure, the maximum strain of rock also increases. When the impact pressure increased from 0.20MPa to 0.35MPa, the maximum strain of the sample increased by 2.36 times. This situation can be attributed to the fact that when the impact pressure is low, the rock absorbs less energy, so that the number of microcracks in the rock is less, and as the impact pressure increases, more energy is used for the initiation of microcracks in the rock [16].

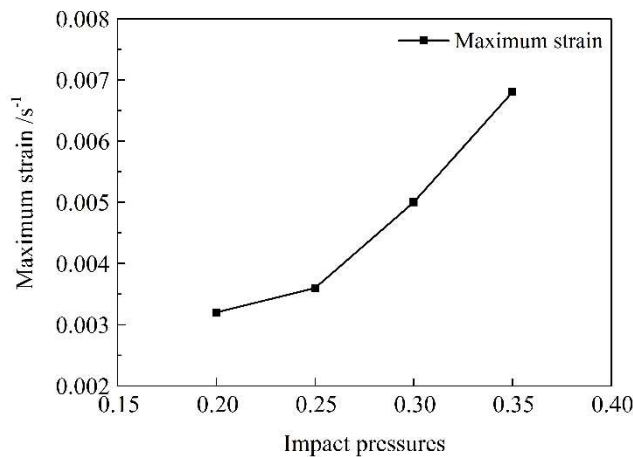


Fig. 4. Relationship between maximum strain and impact pressures.

5. Conclusion

In this paper, the SHPB test device is used to carry out dynamic compression tests on rock samples under four kinds of impact pressures, and the mechanical properties of rocks under dynamic loads are explored. Through the analysis of the test results, the following conclusions are obtained:

- (1) For the same kind of rock, the dynamic stress-strain curves of the samples under different shock gas pressures are similar, With the application of impact load, showing a staged change. With the increase of impact air pressure, the overall change law of the dynamic stress-strain curve of the sample remains unchanged, but its opening range becomes larger, and the curve rises as a whole.
- (2) Under different impact pressures, the dynamic peak stress of rock increases gradually with the increase of shock pressure. Rocks exhibit significant rate effects.
- (3) Because the larger impact pressure is accompanied by more impact energy, the rock will have greater deformation and damage under the larger impact pressure. When the impact pressure was increased from 0.20MPa to 0.35MPa, the maximum strain on time increased by 2.36 times.

References

- [1] Verma HK, Samadhiya NK, Singh M, Goel RK, Singh PK. Blast induced rock mass damage around tunnels. *Tunn Undergr Sp Tech* 2018; 71: 149-158.
- [2] Yang JH, Lu WB, Hu YG, Chen M, Yan P. Numerical simulation of rock mass damage evolution during deep-buried tunnel excavation by drill and blast. *Rock Mech Rock Eng* 2015; 48(5): 2045-2059.
- [3] Yan P, Lu WB, Chen M, Hu YG, Zhou CB, Wu XX. Contributions of in-situ stress transient redistribution to blasting excavation damage zone of deep tunnels. *Rock Mech Rock Eng* 2015; 48: 715-726.
- [4] Xie LX, Lu WB, Zhang QB, Jiang QH, Chen M, Zhao J. Analysis of damage mechanisms and optimization of cut blasting design under high in-situ stresses. *Tunn Undergr Sp Tech* 2017; 66: 19-33.
- [5] Fan Y, Lu WB, YanP, Chen M, Zhang YZ. Transient characters of energy changes induced by blasting excavation of deep-buried tunnels. *Tunn Undergr Space Technol* 2015; 49: 9-17.
- [6] Yang JH, Jiang QH, Zhang QB, Zhao J. Dynamic stress adjustment and rock damage during blasting excavation in a deep-buried circular tunnel. *Tunn Undergr Sp Tech* 2018; 71: 591-604.
- [7] Silva J, Worsley T, Lusk B. Practical assessment of rock damage due to blasting. *Int J Min Sci Techno* 2019; 29(3): 379-385.
- [8] Li XB, Li CJ, Cao WZ, Tao M. Dynamic stress concentration and energy evolution of deep-buried tunnels under blasting loads. *Int J Rock Mech Min Sci* 2018; 104: 131-146.
- [9] Luo Y, Wang G, Li X, Liu TT, Mandal AK, Xu MG, Xu K. Analysis of energy dissipation and crack evolution law of sandstone under impact load. *Int J Rock Mech Min Sci* 2020; 132:104359.
- [10] Shi L, Xu JY. Effect of strain rate on the dynamic compressive mechanical behaviors of rock material subjected to high temperatures. *Mech Mater* 2015; 82: 28-38.
- [11] Li XB, Lok TS, Zhao J. Dynamic characteristics of granite subjected to intermediate loading rate. *Rock Mech Rock Eng* 2005; 38(1): 21-39.
- [12] Wu R, Li H, X Li, Xia X, Liu L. Experimental study and numerical simulation of the dynamic behavior of transversely isotropic phyllite. *Int J Geomech* 2020; 20(8): 04020105.
- [13] Frew DJ, Forrestal MJ, Chen W. A split Hopkinson pressure bar technique to determine compressive stress-strain data for rock materials. *Exp Mech* 2001; 41(1): 40-46.
- [14] Ma HY, Yue CJ, Yu HF, Mei QQ, Chen L, Zhang JH, Zhang YD, Jiang XQ. Experimental study and numerical simulation of impact compression mechanical properties of high strength coral aggregate seawater concrete. *Int J Impact Eng* 2020; 137: 103466.
- [15] He LH, Swain MV. Nanoindentation derived stress-strain properties of dental materials. *Dent Mater* 2007; 23(7): 814-821.
- [16] Kang P, Liu ZP, Zou QL, Wu QH, Zhou JQ. Mechanical property of granite from different buried depths under uniaxial compression and dynamic impact: An energy-based investigation. *Powder Technol* 2020; 362: 729-744.